PhD-thesis 2006

Residual Stress Behaviour in Normal Cooled and Rapid Post-Weld Heat Treated Rail Flash-Butt Welds

David Tawfik

Monash University
Melbourne, Australia

Background

- Flash butt welding: increased use in Australia
- Welds may fail, particularly under high axle loads (haulage of minerals of iron ore and coal)
- Presence of imperfections may act as shear drag at external surfaces -> initiation of fatigue cracks
- Tensile residual stresses increase the risk of these fatigue failures

Background cont'd

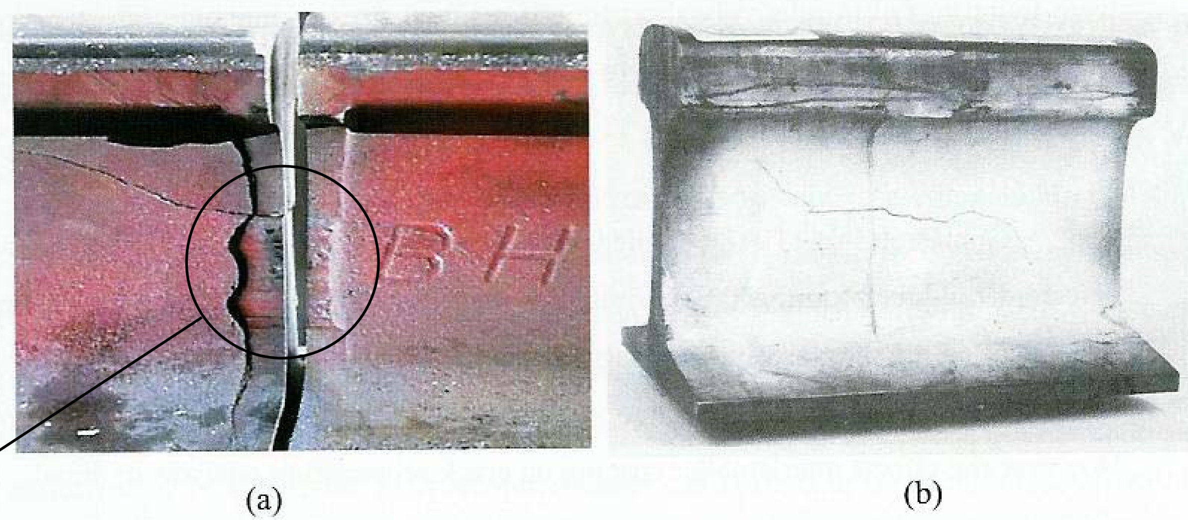

Figure 2.7 Horizontal split web failures (a) Mutton et al, (2003) (b) Marich et al, (1983)

Residual stress level

Objectives

- Investigate thermal stress behavior of normal cooled flash butt welds in pearlitic steel using experimental and numerical techniques

- Compare residual stresses in AS60 and AS68 steels

- Study effects of combined flash butt welding coupled with Rapid Post Weld Heat Treatment (RPWHT) on the residual stress behaviour

- Study effects of combined flash butt welding coupled with Post-Weld Quenching (PWQ) on the residual stress behaviour

Flash butt weld process

Rail ends separated

Preheating-flashing

Upsetting

Trimmed excess weld

Cooled flash butt weld

Figure 2.1 Sequence of flash-butt welding (1) Rail ends separated (2) Preheating-flashing (3) Upset (4) Trimmed excess weld (5) Cooled flash-butt-weld

Experiments

Material:

AS60 pearlitic steel

C : 0.8 %wt

Mn: 0.87 %wt

Si: 0.19 %wt

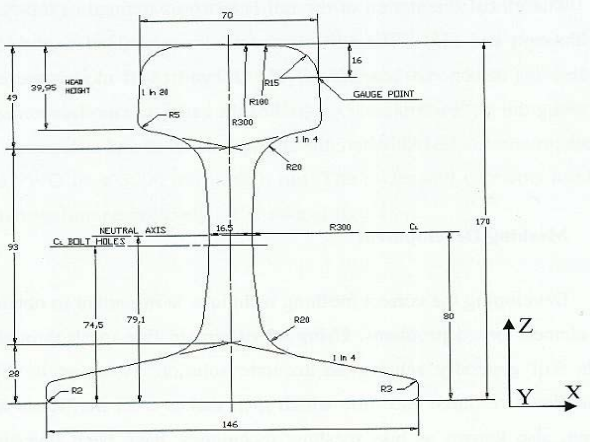

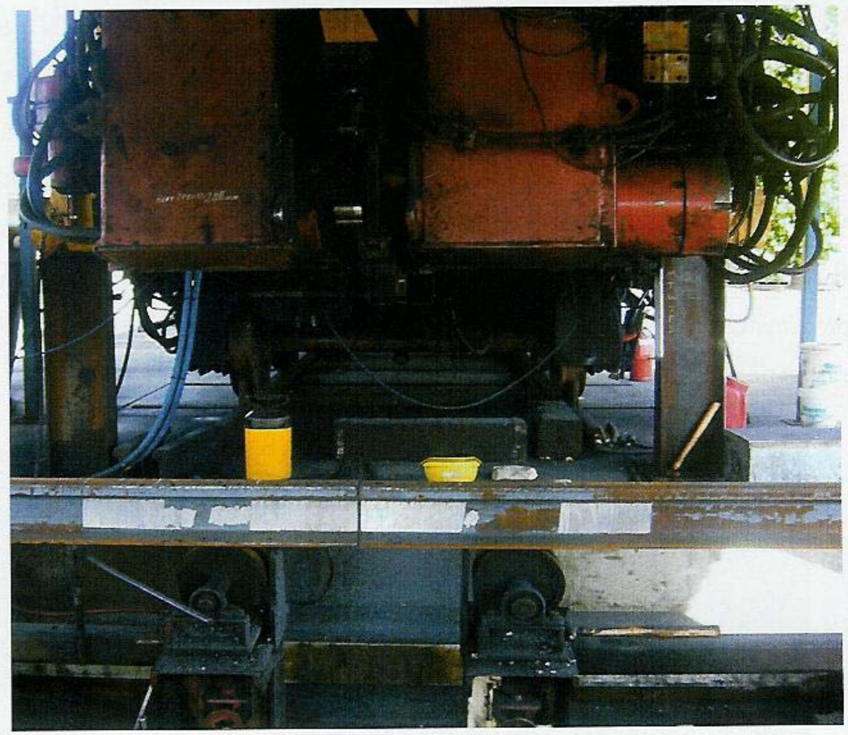

ure 3.8 Plasser mobile flash-butt welder used to produce the AS60 welded rails

CCT-diagram

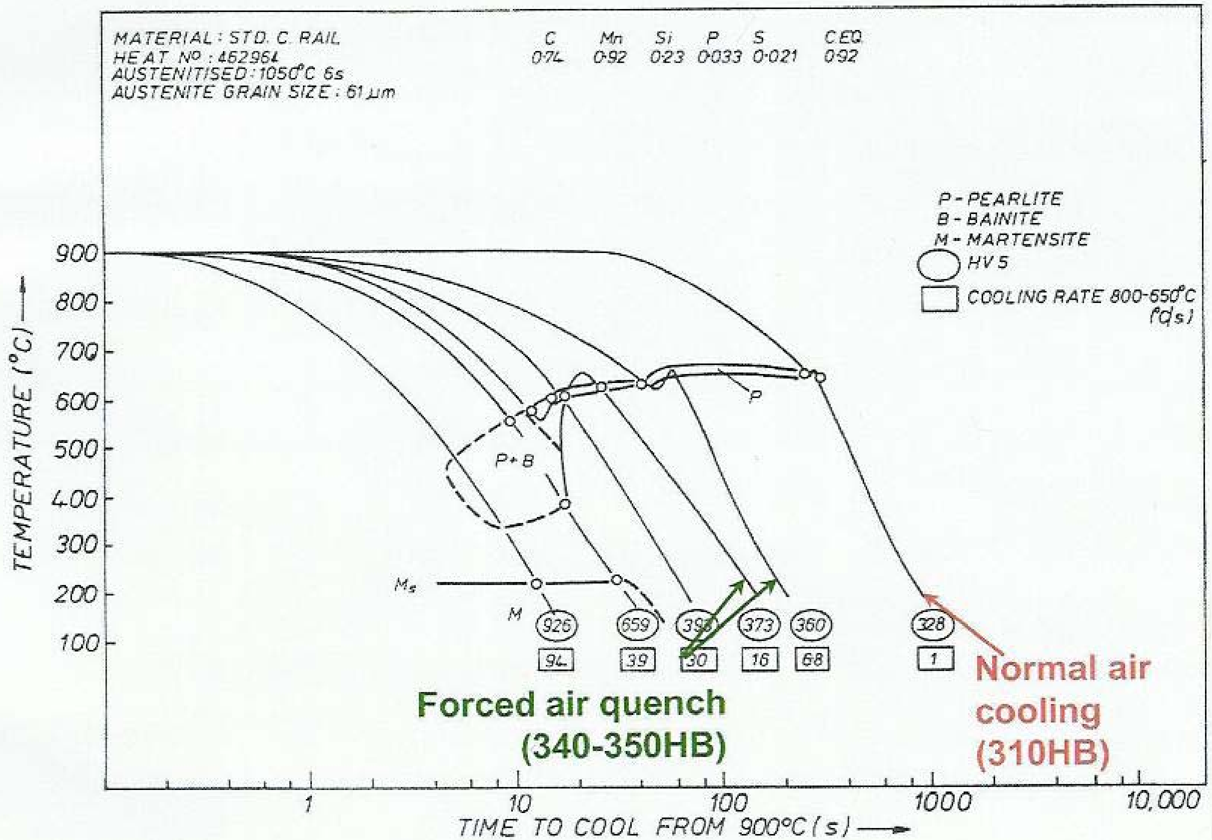

CCT DIAGRAM: STANDARD C RAIL

Experimental setup

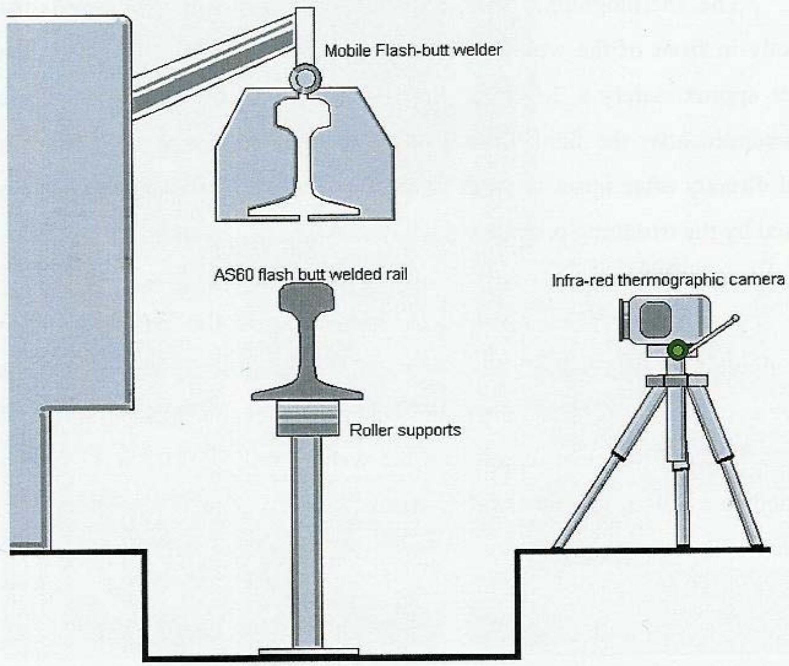

Figure 3.10 Mobile flash-butt welder and thermographic camera schematic setup

Strain measurements

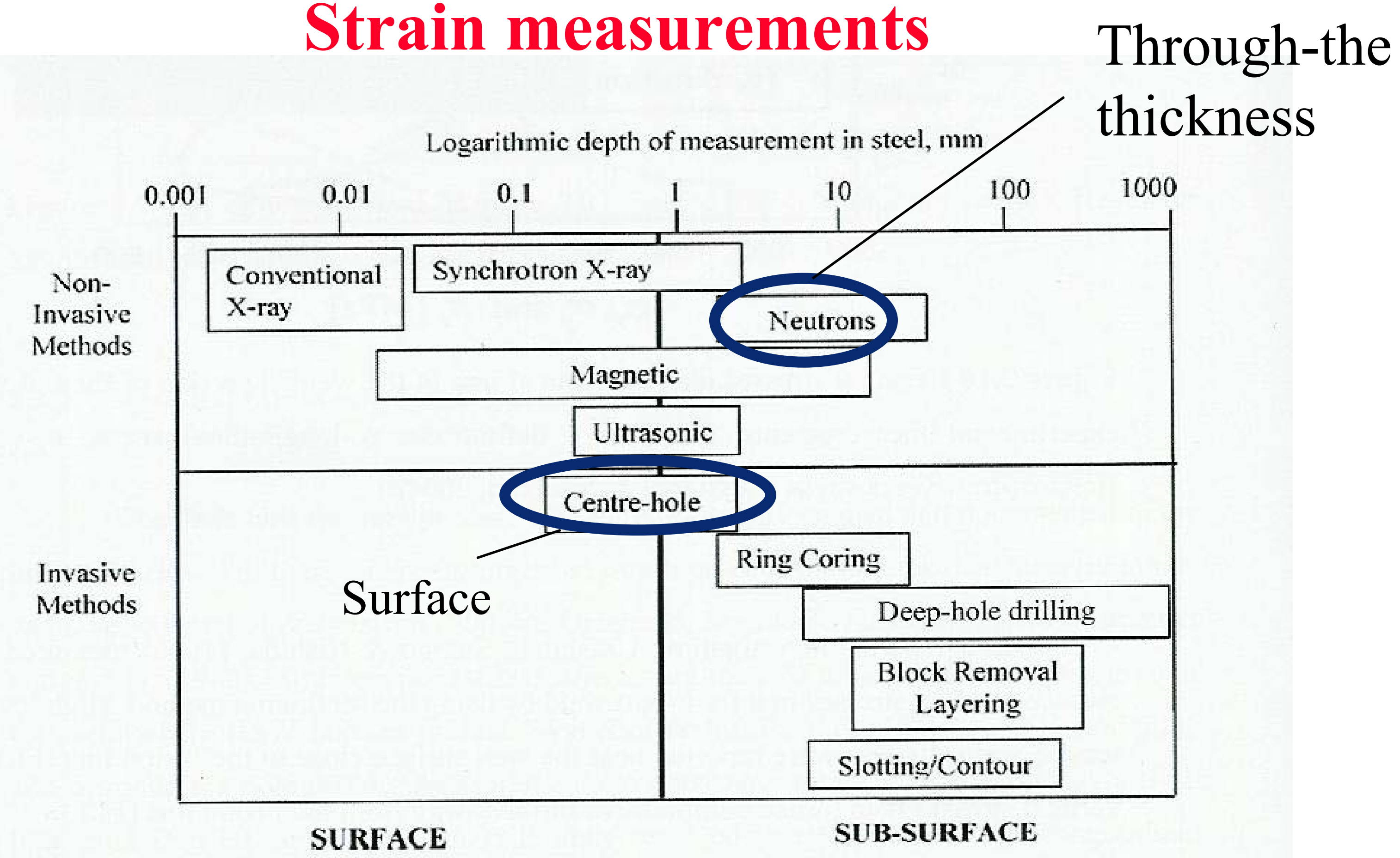

Figure 2.11 Residual stress measurement methods in metals (George & Smith, 2005)

Neutron diffraction measuerments

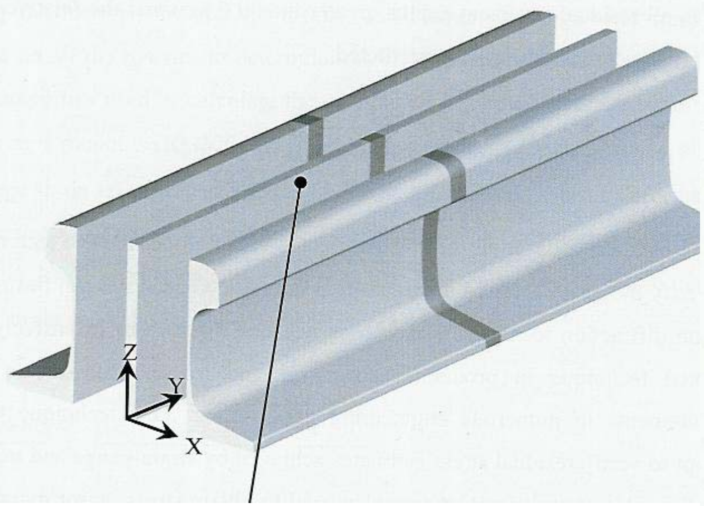

Section for measurement

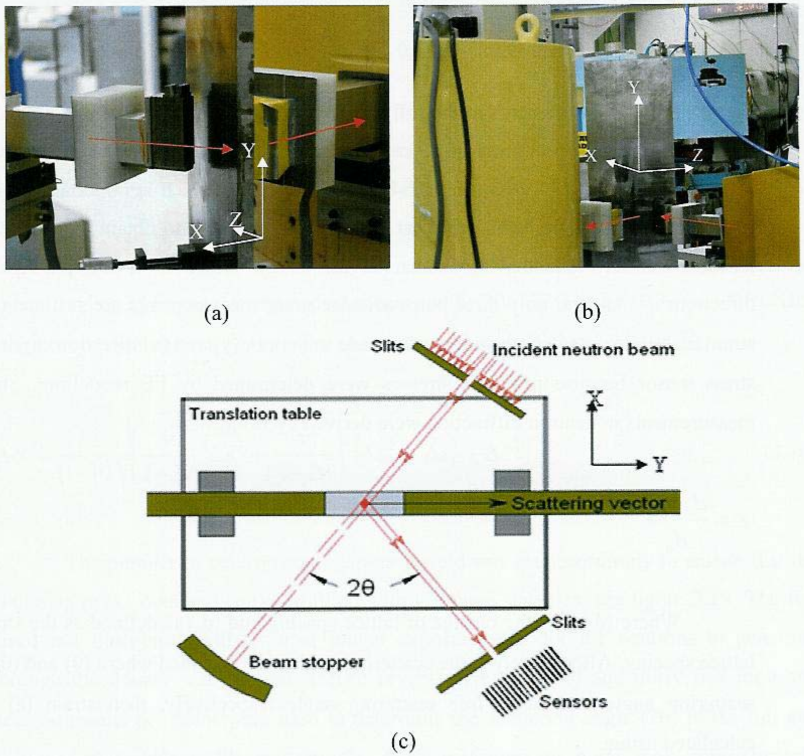

Figure 3.16 Specimen orientation for neutron diffraction measurement in the (a) Vertical (z) (b) Transverse (x) and (c) Longitudinal (y) directions

Rapid Post Weld Heat Treatment

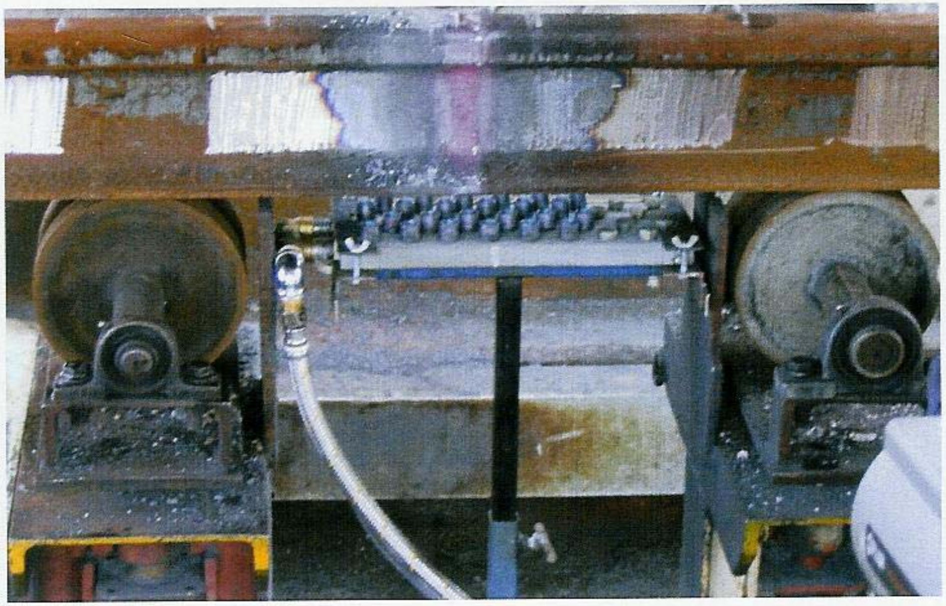

Figure 3.11 Rapid post-weld heat treatment of the rail foot initiated during the post-weld cooling phase of the flash-butt welding process

Finite element modelling

- Use ABAQUS software
- Effects of volume changes associated with pearlitic transformations included (based on exp:s)
- Welding modelled as initial thermal condition (field) immediately after upsetting
- Plasticity modelled with linear kinematic hardening combined with temperature-annealing
- Temperature dependent prop:s from the literature

Residual stress field (normal cooled)

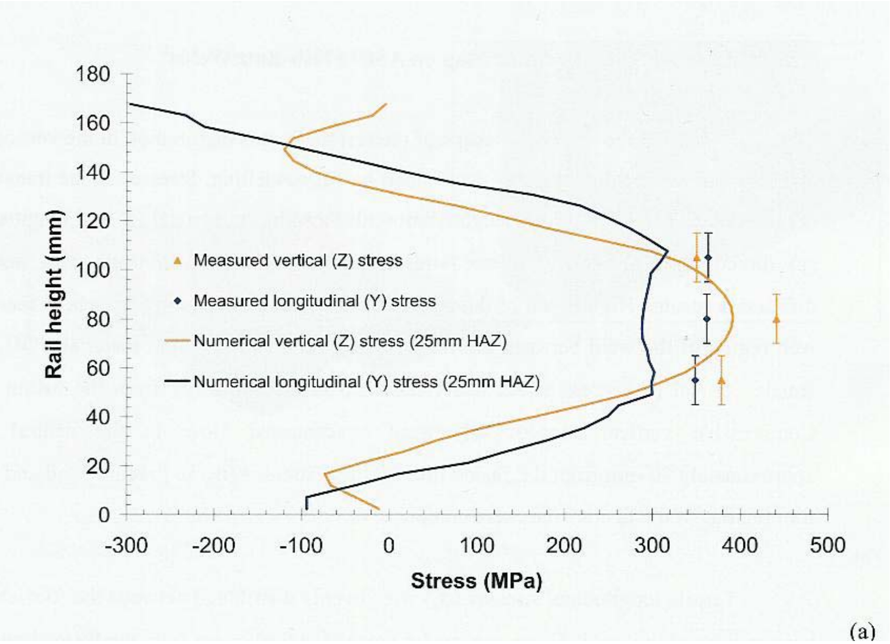

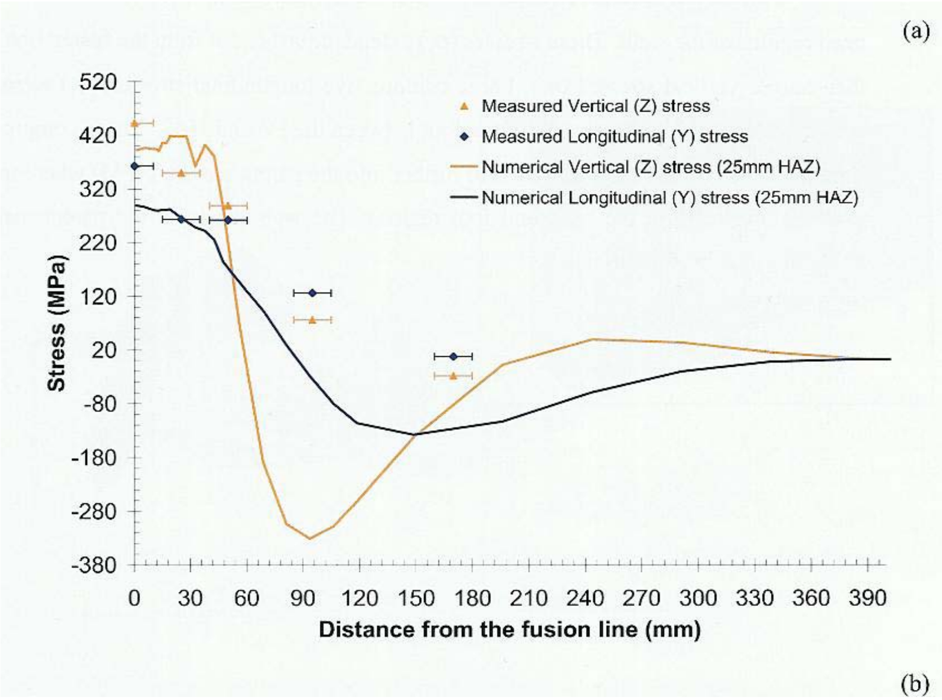

Vertical (z) and longitudinal (y) residual stress
Left: vertical direction Right: longitudinal direction

Residual stress field (normal cooled)

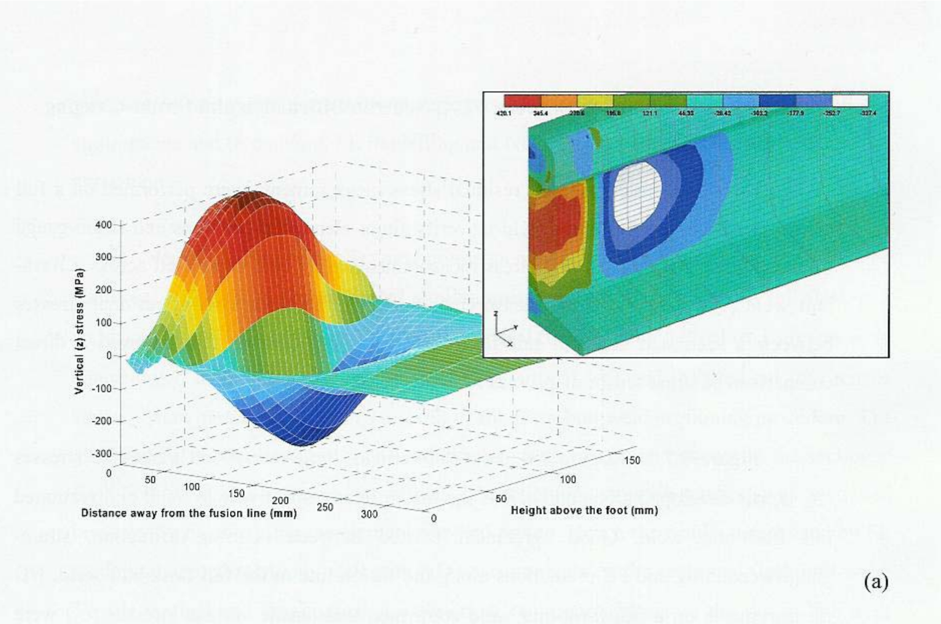

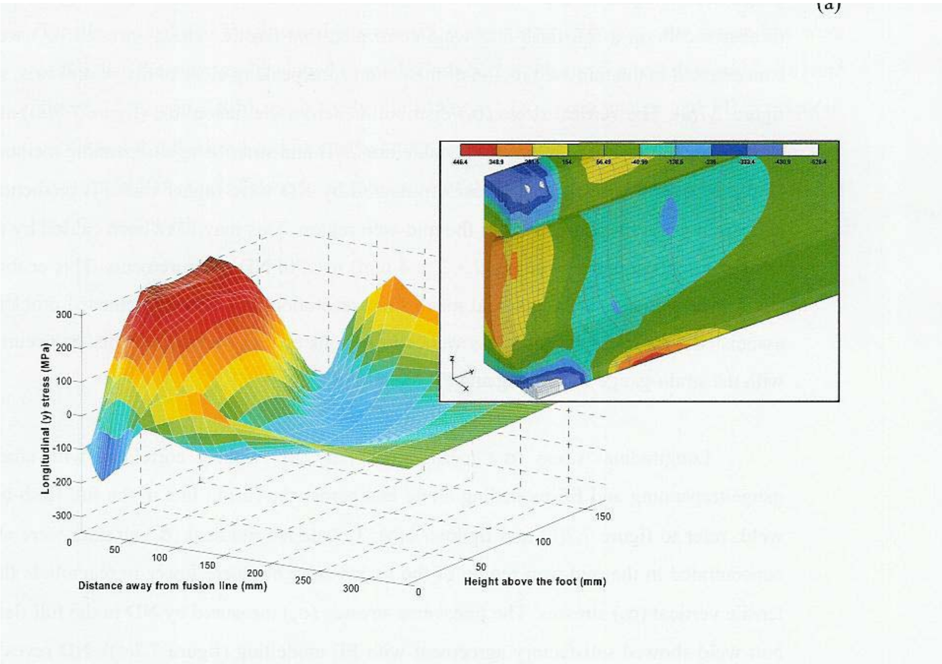

Vertical (z) and longitudinal (y) residual stress

Microstructure, hardness

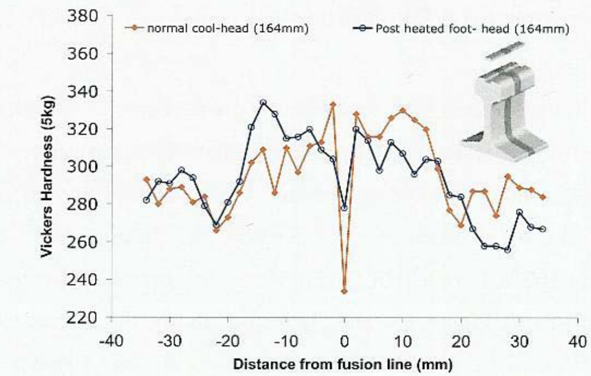

(b)

(a)

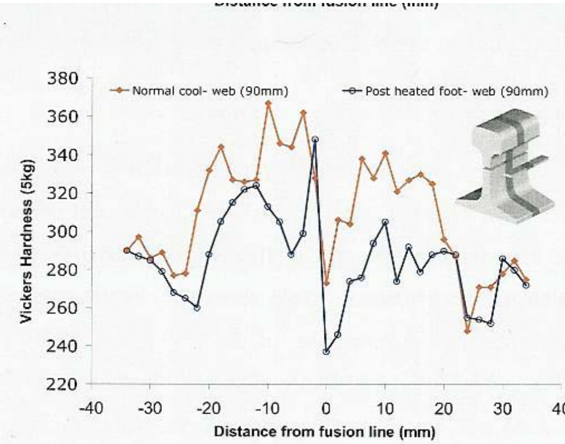

(b)

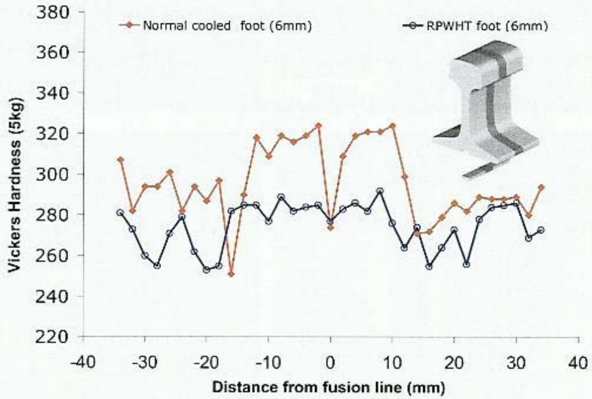

(c)

Hardness measured
in normal condition and after
RPWHT.
Head- upper left
Web – upper right
Foot – lower left

Anders Skyttebol PhD-thesis

Materials testing of rail steel R260 (900A)

- Mechanical properties
- Microstructure evaluation
- Fractography
- Process measurements

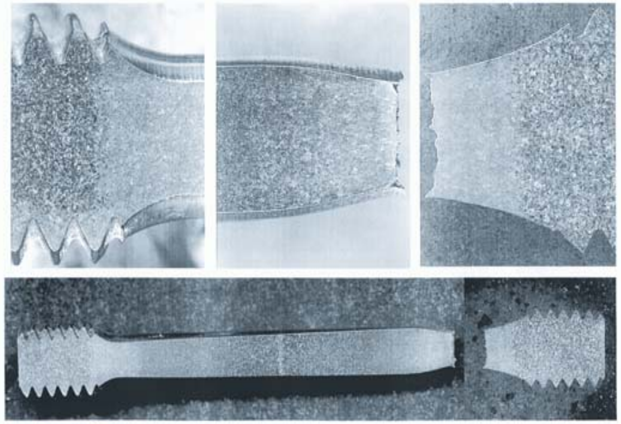

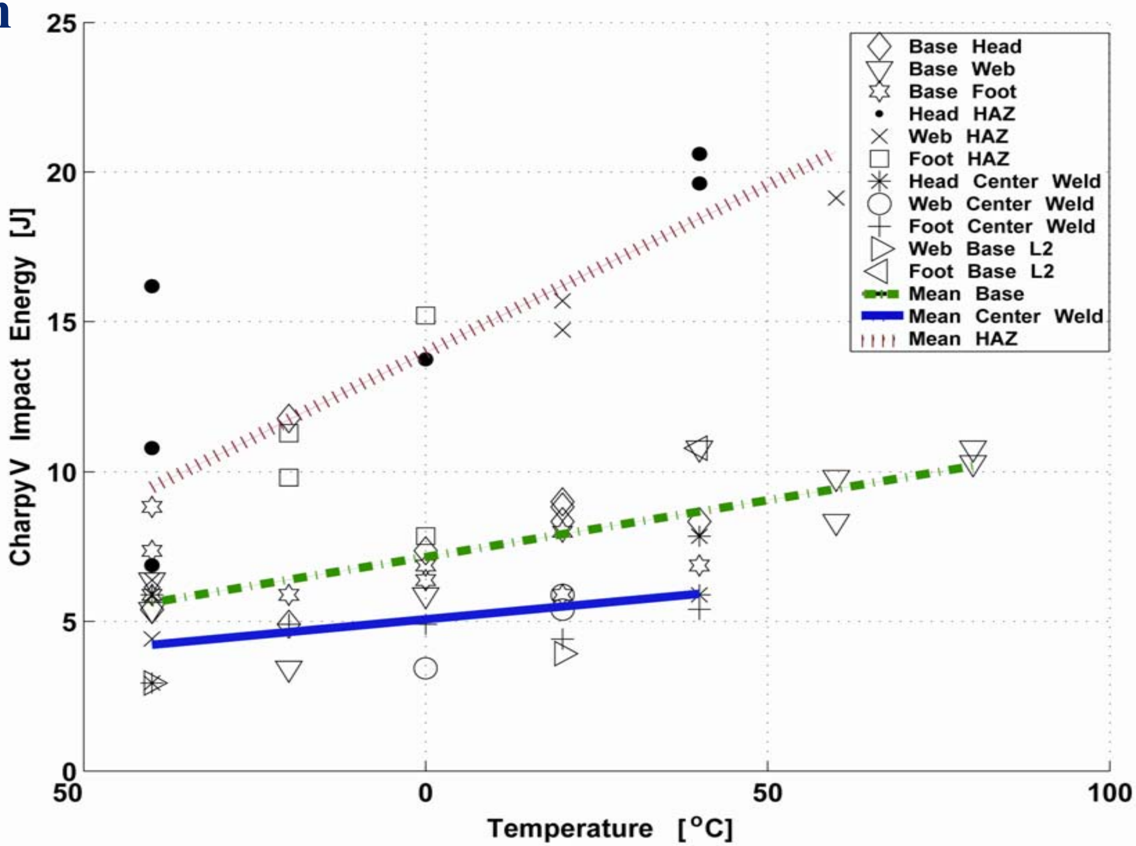

Lamellar pearlite 110 μm | **Globular pearlite 25 μm** | **Ferrite precipitation in grain boundaries 155 μm**

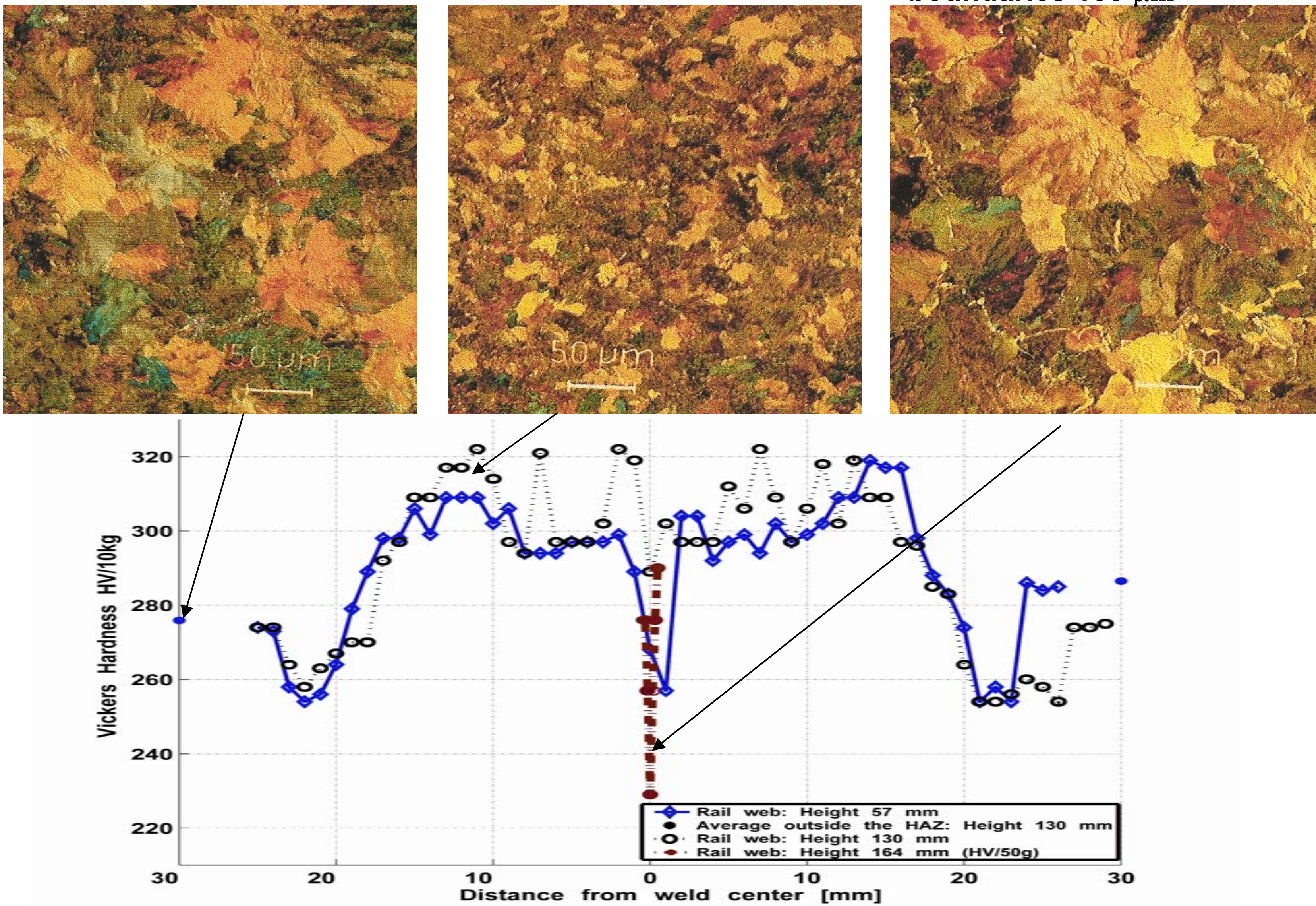

Rapid Post Weld Heat Treatment

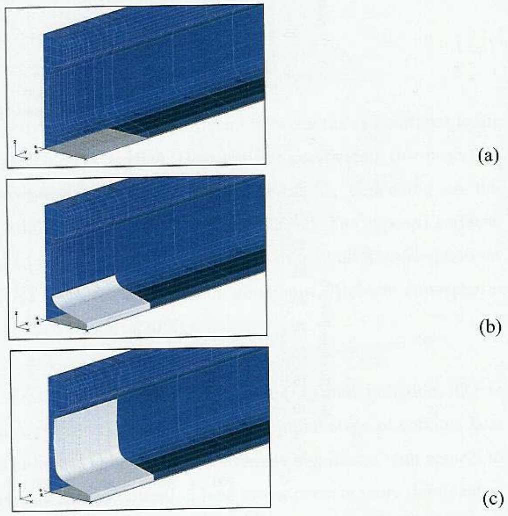

Figure 5.11 Locations of rapid post-weld heat treatments in the weld (a) underneath the foot, RPWHT (A) (b) the entire foot, RPWHT (B) (c) the entire foot and web region, RPWHT (C)

Vary

- Span
- Heat flux intensity
- Region where applied
- Duration
- Initiation time /temp after upsetting

Rapid Post Weld Heat Treatment

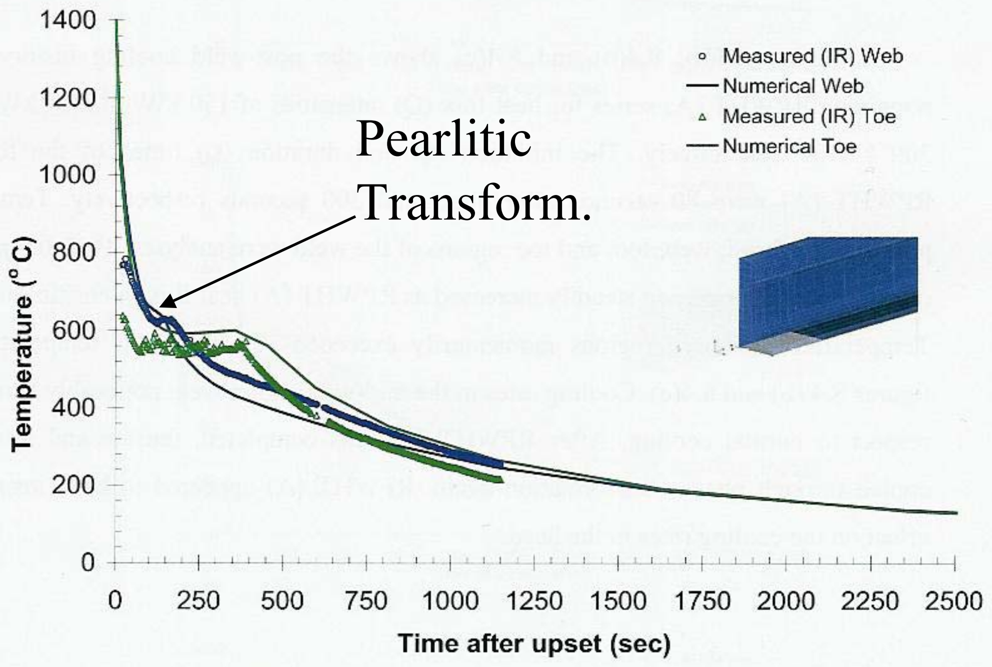

Figure 8.3 Post-weld thermal history for RPWHT (A) determined by infra-red thermography and FE modelling, (Q-120 kW/m^2, t_s-80 sec, t_d-300 sec)

Rapid Post Weld Heat Treatment

Reduction of tensile vertical residual stress

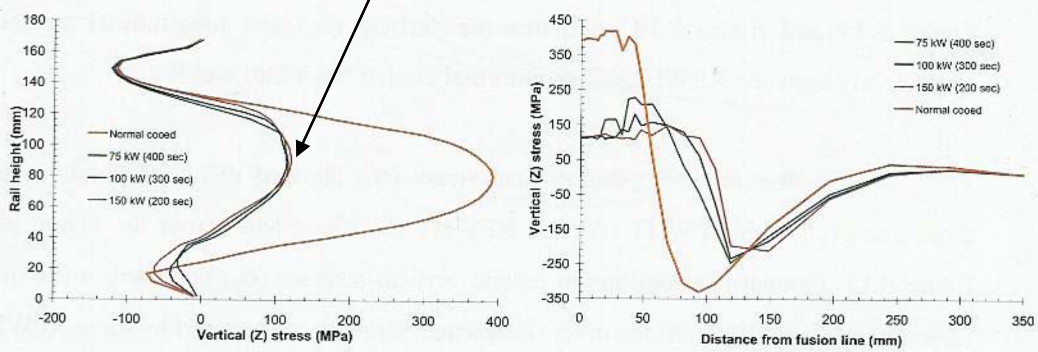

Figure 8.17 Vertical stresses (σ_z) along and across the fusion line between RPWHT (C), (Q-75 kW/m^2, t_d-400 sec; Q-100 kW/m^2, t_d-300 sec; Q-150 kW/m^2; t_d-200 sec; t_s-80 sec) and normal cooled flash-butt welds

Rapid Post Weld Heat Treatment

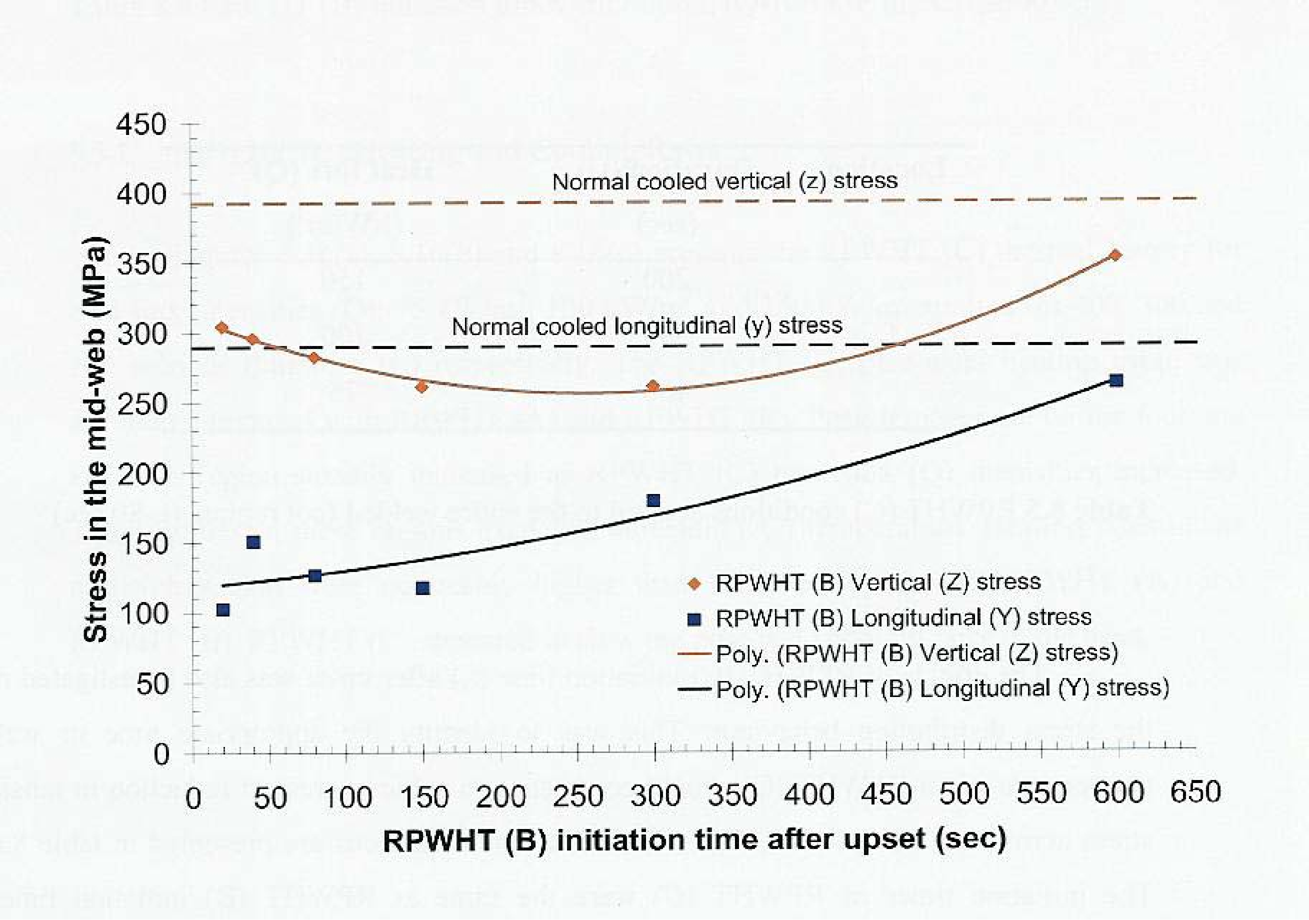

Rapid Post Weld Heat Treatment

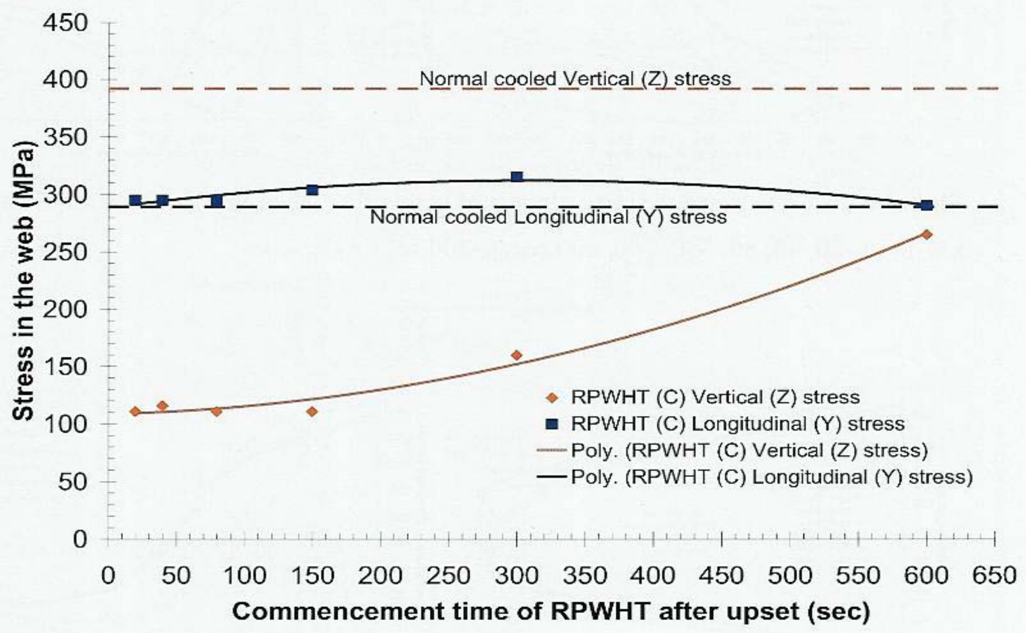

Figure 8.22 Vertical and longitudinal stress (σ_z, σ_y) in the web region for varying RPWHT (C) initiation times, (Q-100 kW/m^2, t_d-300 sec)

Post-Weld Quenching (PWQ)

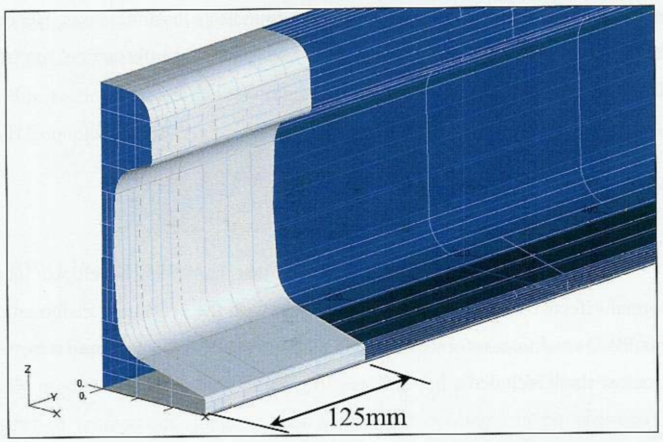

Figure 9.1 PWQ weld surface region, (S-250 mm)

Vary

- Span
- Heat transfer coeff
- Duration time
- Initiation time / temp

Post-Weld Quenching (PWQ)

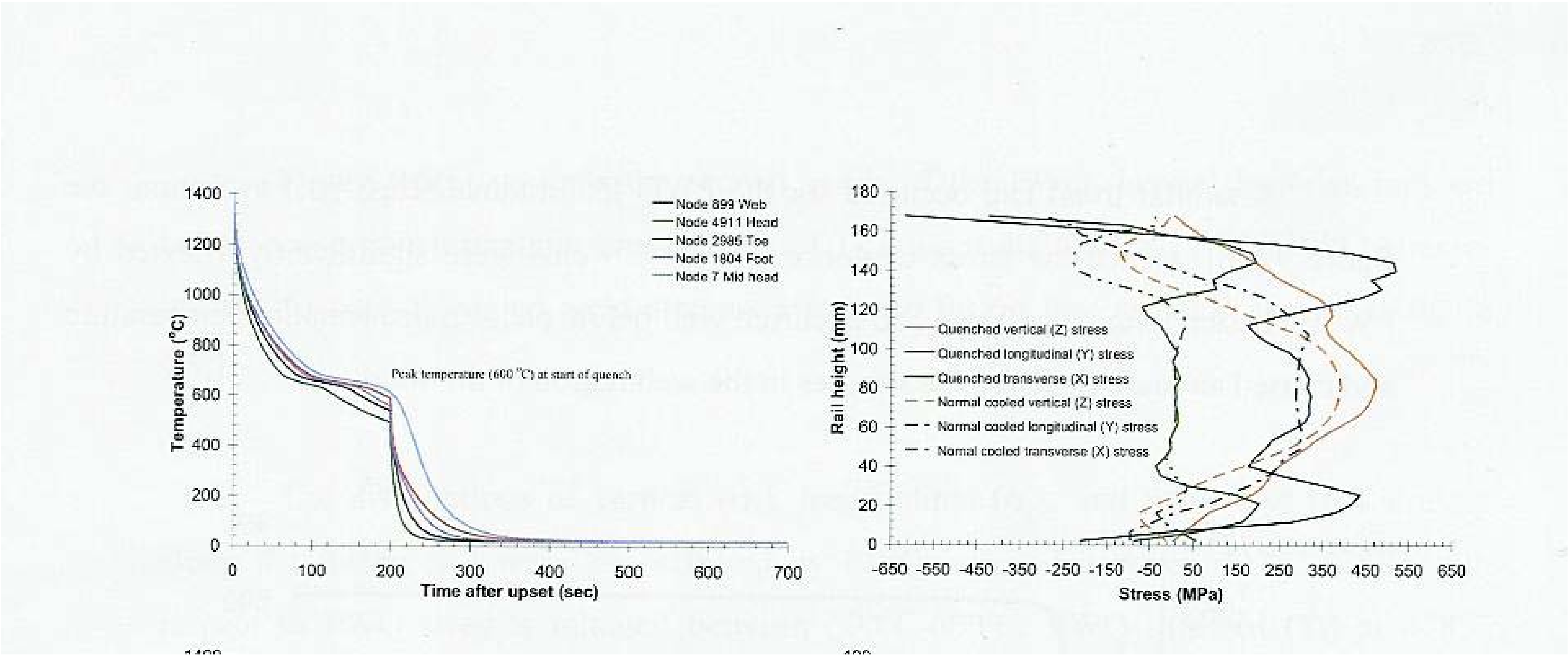

Post-Weld Quenching (PWQ)

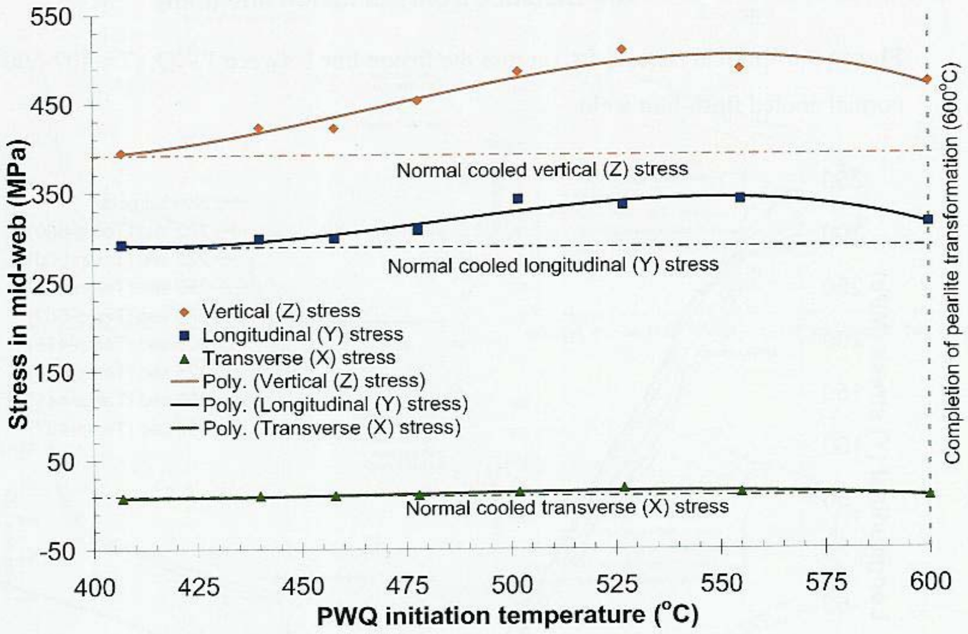

Figure 9.8 Vertical, longitudinal and transverse stress (σ_z, σ_y, σ_x) in the web region for varying PWQ initiation temperatures (T_s)

Conclusions

- Good correlation between FE-calculated and measured (strain gauges and neutron diffraction) residual stress field
- Large tensile residual stresses σ_y and σ_z in the web region
- RPWHT after final upsetting in entire foot resulted in drastic reduction of σ_z (vertical stress). Other RPWHT:s resulted in significant reduction of vertical and longitudinal stresses in web region. RPWHT gives marginally lower hardness.
- PWQ initiated below pearlitic transformation increases vertical and longitudinal stresses.

Anders Skyttebol PhD-thesis
(Stresses as function of rail height)

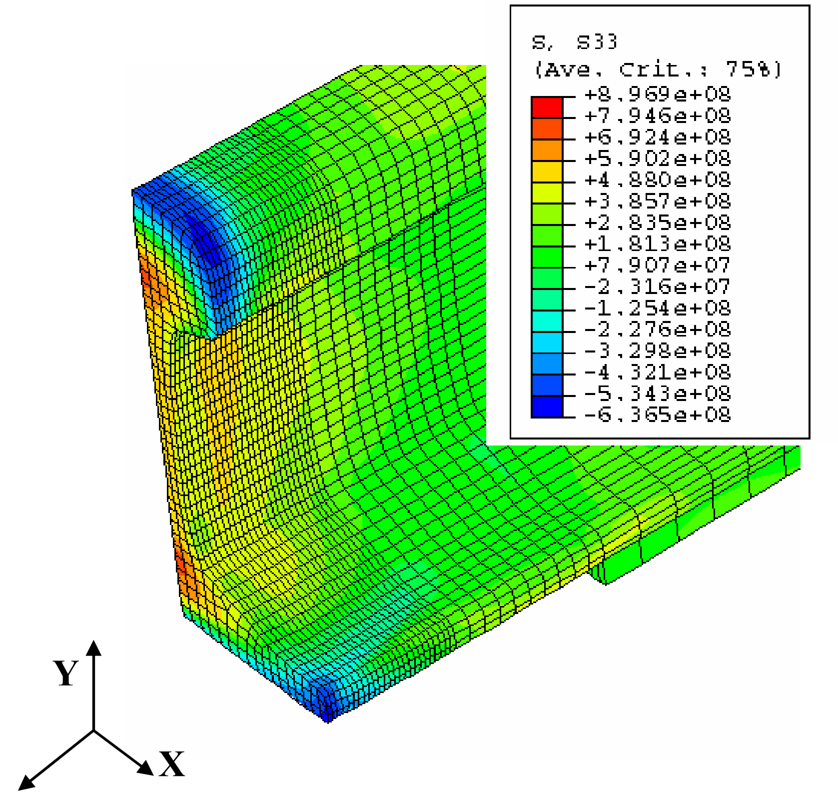

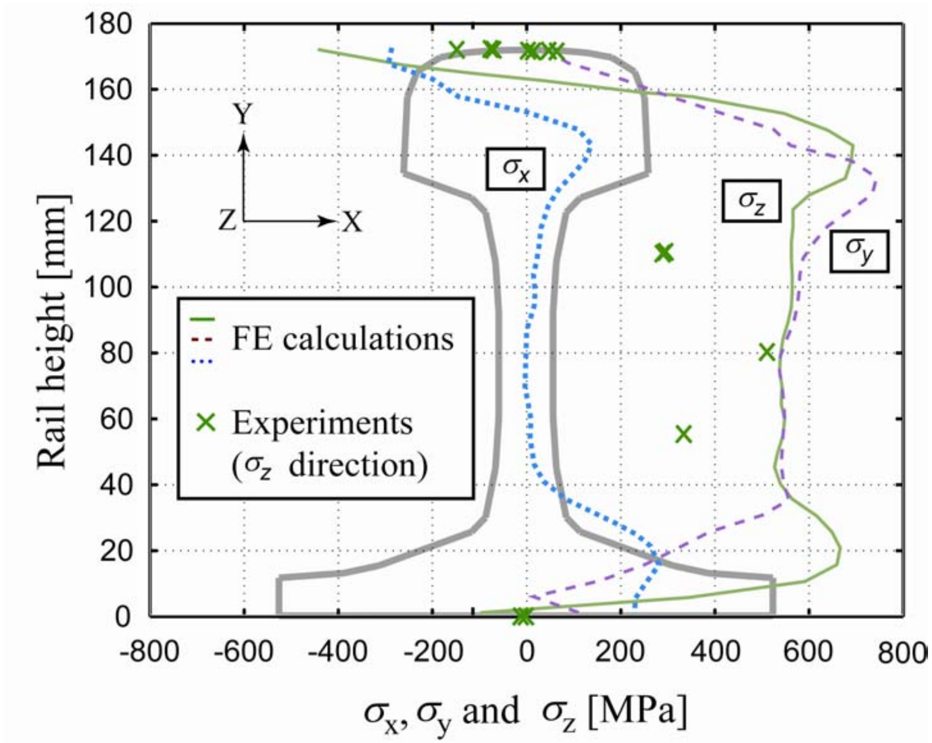

Residual stress field after welding

Residual stresses - Comparison with experiments

Fatigue evaluation for different service conditions

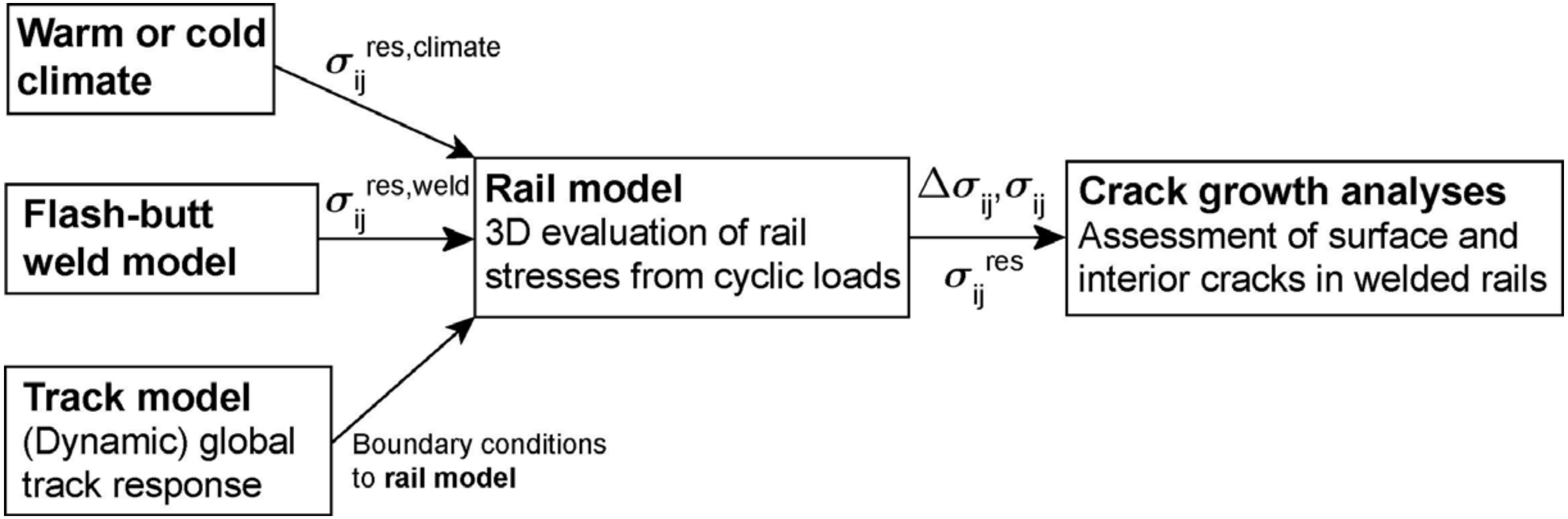

Elastic shakedown after 8 wheel passes

(a): elastic response
(b): elastic shakedown
(c): plastic shakedown
(d): ratchetting

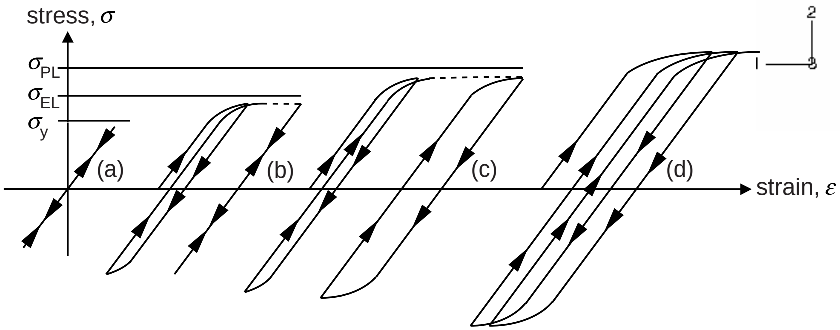

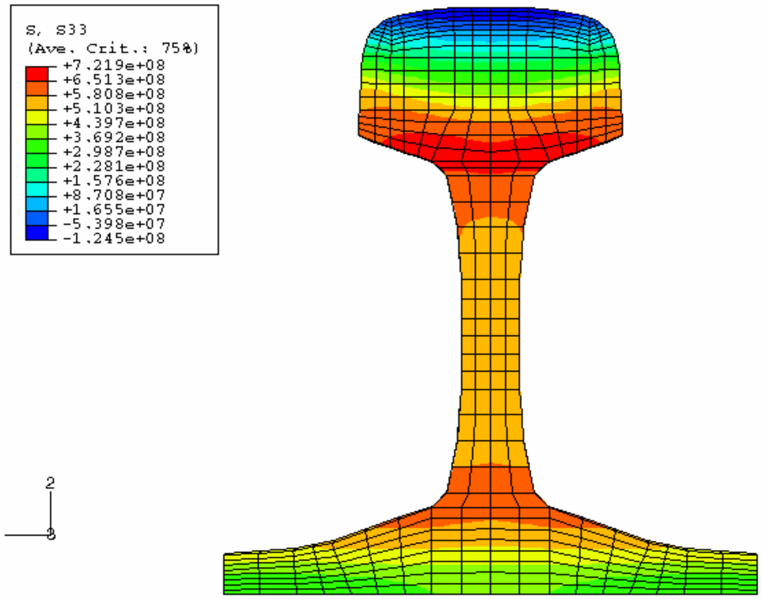

Residual stress in the longitudinal direction after the eighth wheel passage

Stresses from a train pass

- **Data to track and rail models:**
  - Axle load: 30-40 tonnes
  - Hertzian load: p_0=1411 MPa (applied on the rail model)
  - Train speed: 50 km/h
  - Lateral friction factor: 0.10
  - Longitudinal friction factor: 0.35
- **Data to the rail model from a track model analysis:** Cross sectional displacements, or cross sectional rotations
- **Initial conditions to the rail model from the welding FE simulations:**
  - Residual stresses from welding are included in the rail model FE analysis
  - Clamping stress from track laying (Rail is stress free at 20°C)

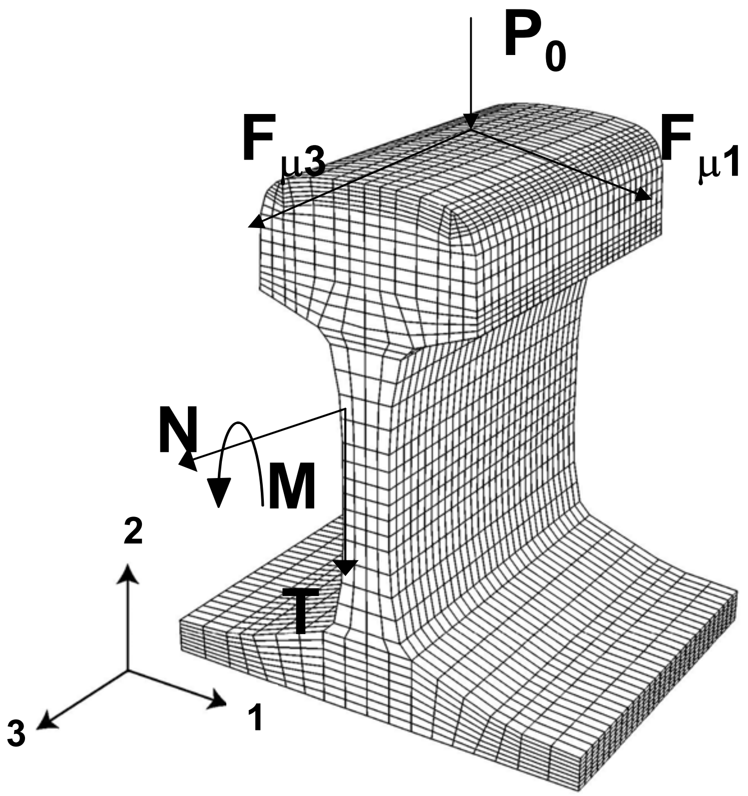

Fatigue crack growth calculations

- **Crack propagation data for rail steel UIC 900A**
  ΔK_{th}=2.0 MPa m$^{1/2}$; C=2.47*10^{-9} ; n=3.33; K_{IC}=40 MPa m$^{1/2}$; A_0= 10 mm^2
- **The welding defects are modelled as cracks in a plate:**
  Example: Surface crack (half-elliptic)

Axle Load [tonnes]	σ_{max} [MPa]	$\Delta\sigma_{33}$ [MPa]	N_f [cycles]	T [°C]	Traffic years:
35	739	46	0.7e6	+20	0.8
30	735	38	7.8e6	+20	9.0
30	661	38	22.0e6	+40	25.3
30	957	38	K_{max}=47>K_{IC}	-40	0

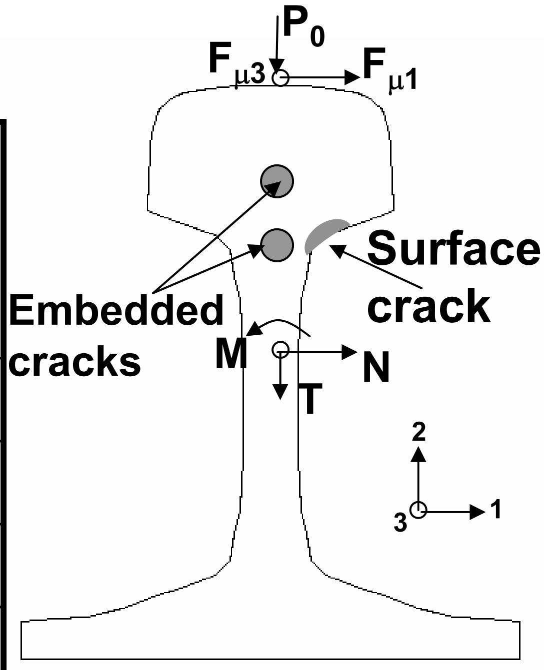

- **$\Delta\sigma_{33}$ is the redistributed stress after eight wheel passages**
- **30-40 tonnes axle load, v = 50 km/h, 870500 axles/year**